BIOCHEMISTRY
including biophysical chemistry & molecular biology

Article

pubs.acs.org/biochemistry

Structure of L-Serine Dehydratase from *Legionella pneumophila*: Novel Use of the C-Terminal Cysteine as an Intrinsic Competitive Inhibitor

James B. Thoden,[†] Hazel M. Holden,*[,†] and Gregory A. Grant*[,‡]

[†]Department of Biochemistry, University of Wisconsin, Madison, Wisconsin 53706, United States

[‡]Department of Developmental Biology and Department of Medicine, Washington University School of Medicine, St. Louis, Missouri 63110, United States

ABSTRACT: Here we report the first complete structure of a bacterial Fe−S L-serine dehydratase determined to 2.25 Å resolution. The structure is of the type 2 L-serine dehydratase from *Legionella pneumophila* that consists of a single polypeptide chain containing a catalytic α domain and a β domain that is structurally homologous to the "allosteric substrate binding" or ASB domain of D-3-phosphoglycerate dehydrogenase from *Mycobacterium tuberculosis*. The enzyme exists as a dimer of identical subunits, with each subunit exhibiting a bilobal architecture. The $[4Fe\text{-}4S]^{2+}$ cluster is bound by residues from the C-terminal α domain and is situated between this domain and the N-terminal β domain. Remarkably, the model reveals that the C-terminal cysteine residue (Cys 458), which is conserved among the type 2 L-serine dehydratases, functions as a fourth ligand to the iron−sulfur cluster producing a "tail in mouth" configuration. The interaction of the sulfhydryl group of Cys 458 with the fourth iron of the cluster appears to mimic the position that the substrate would adopt prior to catalysis. A number of highly conserved or invariant residues found in the β domain are clustered around the iron−sulfur center. Ser 16, Ser 17, Ser 18, and Thr 290 form hydrogen bonds with the carboxylate group of Cys 458 and the carbonyl oxygen of Glu 457, whereas His 19 and His 61 are poised to potentially act as the catalytic base required for proton extraction. Mutation of His 61 produces an inactive enzyme, whereas the H19A protein variant retains substantial activity, suggesting that His 61 serves as the catalytic base. His 124 and Asn 126, found in an HXN sequence, point toward the Fe−S cluster. Mutational studies are consistent with these residues either binding a serine molecule that serves as an activator or functioning as a potential trap for Cys 458 as it moves out of the active site prior to catalysis.

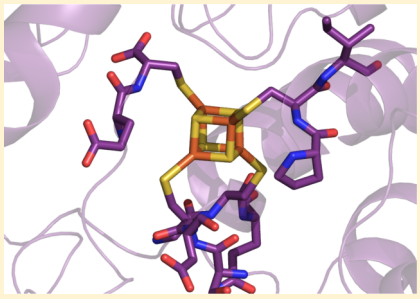

Given that L-serine serves as a major source of one-carbon units for methylation reactions, it is not surprising that its metabolism is a tightly regulated process.[1] Indeed, high rates of serine biosynthesis have been reported in human colon carcinoma, rat sarcoma, and rat hepatoma cell lines, attesting to a possible role in tumor cell growth.[2,3] In many bacteria, defects in the phosphorylated pathway of L-serine production result in auxotrophy,[4,5] whereas high levels of L-serine can be toxic.[6]

All organisms contain enzymes that specifically deaminate L-serine to produce pyruvate and ammonia. In eukaryotes, these enzymes utilize pyridoxal 5′-phosphate (PLP) for activity, and they are believed to function in metabolism by providing pyruvate for gluconeogenesis and the citric acid cycle. Strikingly, in bacteria, the serine dehydratases contain Fe−S clusters rather than PLP.[7−9] Most, if not all bacteria, produce at least one Fe−S L-serine dehydratase, and some, such as *Escherichia coli*, produce several that are differentially expressed.[8,10] The ubiquitous nature of these enzymes attests to their fundamental importance, but it is not known why bacterial L-serine dehydratases utilize an Fe−S cluster rather than PLP. Recent reports suggest that these enzymes play a protective role in guarding against high intracellular L-serine levels that are detrimental to the organism. In *E. coli*, high serine levels interfere with incorporation of alanine into the peptidoglycans at a critical point in cell wall synthesis.[10,11] In some mycobacteria that are missing L-serine dehydratase, high serine levels inhibit growth by blockage of glutamine synthetase,[12] and in *Campylobacteri jejuni*, L-serine dehydratases are essential for host colonization.[13] Importantly, the L-serine dehydratases must function in a manner that does not deplete the levels of L-serine required for viability. They appear to accomplish this task by maintaining a high K_m for L-serine along with a high k_{cat} for efficient turnover.[8,14]

The bacterial Fe−S L-serine dehydratases from *Peptostreptococcus asaccharolyticus*[15] and *E. coli*[8] have been shown to contain a diamagnetic $[4Fe\text{-}4S]^{2+}$ cluster in which three of the irons are thought to be ligated by cysteine residues whereas the fourth presumably interacts with the substrate, similar to that observed in aconitase.[16] A potential catalytic mechanism for L-serine dehydratase is shown in Scheme 1. The model is based on mechanistic studies with aconitase and other 4Fe-4S dehydratases.[8,9,14] Most nonredox 4Fe-4S proteins contain a cubane structure in which three of the four iron atoms are ligated to

Received: October 3, 2014
Revised: November 5, 2014
Published: November 7, 2014

   dx.doi.org/10.1021/bi501253w | *Biochemistry* 2014, 53, 7615−7624

Scheme 1

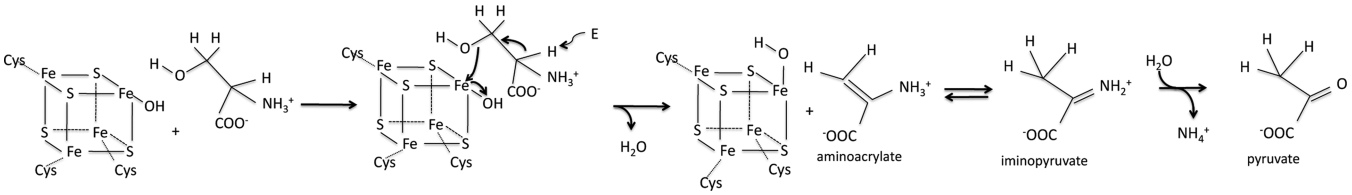

protein cysteine residues. Using aconitase as a model, the fourth iron is generally described as the catalytic metal that is ligated to water and interacts directly with the substrate according to the general mechanism depicted in Scheme 1. A catalytic base extracts a proton from the α carbon, and the Fe−S cluster acts as a Lewis acid, which coordinates the leaving hydroxyl group of the substrate. The aminoacrylate dehydration product is protonated at the β carbon to form iminopyruvate that is subsequently rehydrated with the loss of ammonia to form pyruvate. Site-directed mutagenesis studies with the *Legionella pneumophila* L-serine dehydratase have revealed that the critical cysteines are found in a C-X_{41}-C-X_{10}-C sequence pattern.[14]

At least four types of Fe−S L-serine dehydratases that differ in their domain content and arrangement have been identified.[17] They all contain a catalytic or α domain that harbors the binding site for the Fe−S cluster as well as a β domain whose function has not yet been completely defined. In the type 1 enzymes, the α and β domains are found on separate polypeptide chains, whereas in types 2−4, they are located on a single polypeptide chain.[17,18] In the type 2 and 4 enzymes, the β domain is found at the N-terminus, whereas in the type 3 enzymes, the β domain is located at the C-terminus. A partial structure of the *L. pneumophila* L-serine dehydratase representing the β domain alone (residues 11−161), determined in 2006 by the Midwest Center for Structural Genomics, revealed that its fold had a molecular architecture similar to that of the "allosteric substrate binding" or "ASB" domain observed in some D-3-phosphoglycerate dehydrogenases.[14] The D-3-phosphoglycerate dehydrogenases function in metabolism by catalyzing the first and rate-limiting step in serine biosynthesis.[1] The β domains of type 1, 3, and 4 L-serine dehydratases contain an additional segment of polypeptide that appears to be similar to the "ACT" domain also found in the D-3-phosphoglycerate dehydrogenases. In addition, type 1 and 3 L-serine dehydratases require potassium for activity, whereas the type 2 enzymes do not.[18]

The ASB domain in D-3-phosphoglycerate dehydrogenase functions in enzyme regulation by binding substrate, and possibly phosphate, which act as allosteric effectors.[19,20] It is thought that the ASB domain plays a similar role in the L-serine dehydratases by binding serine as an allosteric ligand. Activation by L-serine binding at a second, noncatalytic site has been demonstrated by kinetic analysis of the type 2 enzyme from *L. pneumophila*, although the location of the effector binding site has not yet been directly demonstrated to reside in the β domain.[18,21] The bacterial Fe−S L-serine dehydratases represent only the second group of proteins in which ASB domains have been found.[17] Interestingly, both the L-serine dehydratases and the D-3-phosphoglycerate dehydrogenases are involved in some aspect of L-serine metabolism.

Here we report the first complete structure of the *L. pneumophila* L-serine dehydratase determined to 2.25 Å resolution. Each subunit of the dimeric enzyme adopts a distinctly bilobal architecture with the $[4Fe\text{-}4S]^{2+}$ cluster situated between the N- and C-terminal domains. Remarkably, the model reveals that the C-terminal cysteine residue, which is conserved among the type 2 L-serine dehydratases, functions as a ligand to the iron−sulfur cluster through a "tail in mouth" configuration. The molecular architecture described herein serves as a paradigm for the bacterial L-serine dehydratases in general.

MATERIALS AND METHODS

Cloning of the Gene Encoding Serine Dehydratase. The gene encoding *L. pneumophila* L-serine dehydratase was cloned from genomic DNA obtained from the American Type Culture Collection as previously described.[14] It was placed between the BamHI and HindIII sites of pSV281, which provided a hexahistidine tag at the N-terminus of the protein after expression.

Protein Expression and Purification. BL21 DE3 cells containing the plasmid were grown in lysogeny broth medium supplemented with kanamycin at 37 °C with shaking until an optical density of 0.5−0.7 was reached at 600 nm. Protein expression was induced via the addition of 3 mM isopropyl β-D-1-thiogalactopyranoside, and the cells were grown until an optical density of 1−3 was reached at 600 nm. The cells were recovered by centrifugation, suspended in buffer [50 mM MOPS (pH 7.0) or 100 mM potassium phosphate (pH 7.0)], and lysed by sonication in an anaerobic chamber in the presence of 0.16 mg/mL lysozyme and then treated with 5 mg of DNAase after being stirred for 10 min. Protein was purified in the anaerobic chamber on a Talon Cobalt metal affinity column using standard procedures.[14,21] Mutant proteins were prepared by PCR as previously described[22] and purified in the same manner that was used for the wild-type enzyme.

Kinetic Analysis. Activity was measured by following the absorbance of product (pyruvate) formation at 250 nm.[14] The concentration of the active enzyme was determined from the charge transfer absorbance of the Fe−S center at 400 nm using an extinction coefficient of 13750 M^{-1} cm^{-1}. The kinetic parameters, k_{cat} and K_m, were determined by fitting the L-serine concentration-dependent plot to the cooperative Michaelis−Menten equation

$$v = (V/[S]^n)/(K_m{}^n + [S]^n) \quad (1)$$

where v is the velocity as a function of substrate concentration, V is the maximal velocity, [S] is the substrate concentration, K_m is the Michaelis constant, n is the Hill coefficient, and k_{cat} is $V/[E_t]$. Double-reciprocal plots were fit by linear regression analysis, which yielded values for the slopes. Slope replots and plots of velocity versus inhibitor concentration at a constant substrate concentration were produced as described by Segel.[23] Slope replots were fit either by linear regression analysis or in the case of D-serine to a second-degree polynomial. The values for K_i were estimated graphically where the x-axis intercept

dx.doi.org/10.1021/bi501253w | *Biochemistry* 2014, 53, 7615−7624

equals $-K_i$. The data points in plots of velocity versus inhibitor concentration were connected from point to point using the smooth fit function of Kaleidograph and are used only to show either linear or plateauing functionality. Linearity indicates that the velocity can be driven to zero at an infinite inhibitor concentration, consistent with simple competitive inhibition. A plateau demonstrates that activity cannot be driven to zero at an infinite inhibitor concentration indicating partial inhibition.

Size Exclusion Chromatography. Protein (8−10 mg/mL) isolated in the anaerobic chamber was applied to a 1.6 cm × 100 cm column of Sephacryl S-200 at ambient room atmosphere and developed with 50 mM MOPS buffer (pH 7.0) that had been deoxygenated in the anaerobic chamber. Fractions were assayed for catalytic activity, and the absorbance at 280 nm was measured.

Protein Expression and Purification for X-ray Diffraction Analysis. The pSV281-*lp*LSD plasmid was used to transform Rosetta2(DE3) *E. coli* cells (Novagen). The cultures were grown in M9 medium supplemented with kanamycin and chloramphenicol at 37 °C with shaking until an optical density of 1.0 was reached at 600 nm. Methionine biosynthesis was suppressed by the addition of lysine, threonine, phenylalanine, leucine, isoleucine, valine, and selenomethionine, and 10 mg/L ferrous ammonium sulfate was also added. After an additional 30 min, the flasks were cooled to room temperature, and protein expression was initiated by addition of isopropyl β-D-1-thiogalactopyranoside to a final concentration of 1 mM. The cells were allowed to express protein for 18 h before being harvested.

Protein purification was performed in a COY anaerobic chamber at ambient temperature. The cells were lysed using 0.2 mg/mL lysozyme in standard lysis buffer [50 mM sodium phosphate, 200 mM NaCl, and 20 mM imidazole (pH 8)]. After cell lysis was complete, 0.05 mg/mL DNaseI was added for nucleotide degradation. The lysed cells were subsequently sealed in centrifuge bottles and spun at 45000*g* for 30 min. The supernatant was loaded onto a Ni-NTA column, and after being rigorously washed, the protein was eluted with 50 mM sodium phosphate, 200 mM NaCl, and 250 mM imidazole (pH 8). The sample was dialyzed against 10 mM Tris-HCl (pH 8.0) and 200 mM NaCl. After dialysis, the protein concentration was adjusted to approximately 10 mg/mL based on an extinction coefficient of 2.16 mg^{-1} mL cm^{-1} at 280 nm. Dithiothreitol was added to a final concentration of 8 mM. The Fe−S cluster was reconstituted by adding an 8-fold molar excess of $FeCl_3$ dropwise (100 mM stock) over 15 min, followed by a similar addition of Na_2S. The mixture was allowed to stir for 5 h, followed by dialysis against 10 mM Tris-HCl (pH 8.0) and 200 mM NaCl. The solution was diluted with 3 volumes of 50 mM CHES (pH 9) and loaded onto a DEAE-Sepharose column that had been equilibrated in the same buffer (pH 9). The protein was eluted with a linear gradient from 0 to 800 mM NaCl and dialyzed against 10 mM Tris-HCl (pH 8.0) and 200 mM NaCl. The final protein concentration was 15 mg/mL.

Crystallization. Crystallization conditions were initially surveyed in a COY anaerobic chamber at ambient temperature by the hanging drop method of vapor diffusion using a laboratory-based sparse matrix screen. Single crystals were subsequently grown via vapor diffusion against 100 mM homopipes (pH 5.0), 9−13% poly(ethylene glycol) 3400, and 200 mM tetramethylammonium chloride. The crystals grew to maximal dimensions of ∼0.4 mm × 0.4 mm × 0.05 mm in 2 weeks. They belonged to space group $P3_121$ with the following unit cell dimensions: $a = b = 81.4$ Å, and $c = 267.5$ Å. There was one dimer in the asymmetric unit.

Structural Analysis. Prior to X-ray data collection, the crystals were transferred to a cryoprotectant solution containing 20% poly(ethylene glycol) 3400, 15% ethylene glycol, 250 mM NaCl, 250 mM tetramethylammonium chloride, and 100 mM homopipes (pH 5.0). X-ray data were collected at the Structural Biology Center beamline 19-BM at a wavelength of 0.9794 Å (Advanced Photon Source). The X-ray data were processed and scaled with HKL3000.[24] Relevant X-ray data collection statistics are listed in Table 1.

Table 1. X-ray Data Collection Statistics

	selenomethionine-labeled enzyme
resolution limits	30.0−2.25 (2.29−2.25)[b]
no. of independent reflections	49999 (2399)
completeness (%)	99.7 (97.8)
redundancy	9.0 (6.3)
avg I/avg $\sigma(I)$	37.8 (3.6)
R_{sym} (%)[a]	9.5 (47.3)

[a] $R_{sym} = (\sum|I - \bar{I}|/\sum I) \times 100$. [b] Statistics for the highest-resolution bin are given in parentheses.

The structure of the protein was determined via single-wavelength anomalous dispersion. Analysis of the X-ray data measured from the selenomethionine-labeled crystals with SHELXD revealed 32 selenium atoms.[25,26] Protein phases were calculated using these sites with SHELXE[26] followed by solvent flattening and averaging with RESOLVE.[27,28] An initial model was built and subsequently refined against the SAD X-ray data. Iterative rounds of model building with COOT[29] and refinement with REFMAC[30] reduced the R_{work} and R_{free} to 19.8 and 25.8%, respectively, from 30 to 2.25 Å resolution. Model refinement statistics are listed in Table 2.

Table 2. Refinement Statistics

resolution limits (Å)	30.0−2.25
overall R factor[a] (%)/no. of reflections	20.1/49929
working R factor (%)/no. of reflections	19.8/47391
free R factor (%)/no. of reflections	25.8/2538
no. of protein atoms	6762
no. of heteroatoms	222
average B value (Å^2)	
protein atoms	44.8
ligand	32.5
solvent	42.7
weighted root-mean-square deviation from ideality	
bond lengths (Å)	0.015
bond angles (deg)	1.8
planar groups (Å)	0.007
Ramachandran regions (%)[b]	
most favored	90.6
additionally allowed	9.0
generously allowed	0.4
disallowed	0.0

[a] R factor = $(\sum|F_o - F_c|/\sum|F_o|) \times 100$, where F_o is the observed structure factor amplitude and F_c is the calculated structure factor amplitude. [b] Distribution of Ramachandran angles according to PROCHECK.[32]

dx.doi.org/10.1021/bi501253w | *Biochemistry* 2014, 53, 7615−7624

RESULTS AND DISCUSSION

Overall Molecular Architecture of the Fe−S L-Serine Dehydratase. A previous report on an L-serine dehydratase from *E. coli* indicated that it exists as a dimer in solution.[8] Crystals used in this investigation belonged to the space group $P3_121$ with two subunits in the asymmetric unit. To confirm the quaternary structure of the *L. pneumophila* enzyme, we used size exclusion chromatography. Chromatography of the purified enzyme on a Sephacryl S-200 column showed a single main peak with a trailing shoulder (Figure 1). After elution from the

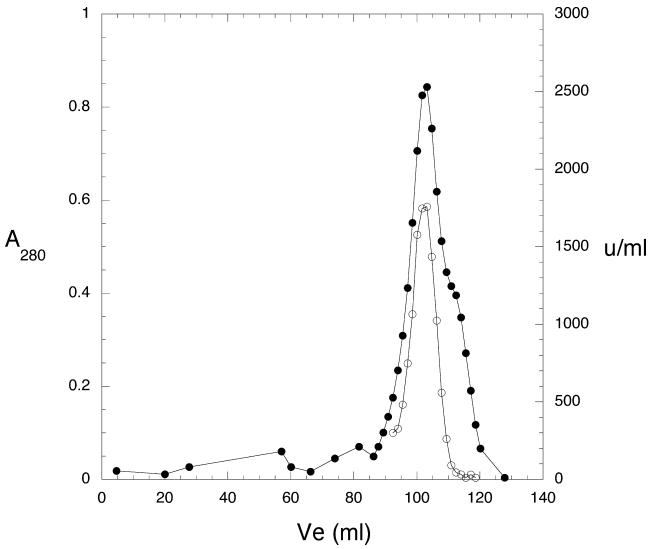

Figure 1. Size exclusion chromatography of the *L. pneumophila* dehydratase. The enzyme was run on a 1.6 cm × 100 cm column of Sephacryl S-200. The absorbance at 280 nm (●) and the enzyme activity (○) are plotted as a function of elution volume.

column, the enzyme retained significant activity that corresponded to the main absorbance peak. The molecular weight of the main peak was determined to be 95500 and that of the shoulder to be approximately 56200. These molecular weights correspond well to the calculated molecular weights of 98952 and 49476 for dimeric and monomeric molecules, respectively. This is consistent with a monomer−dimer equilibrium under the conditions used for the chromatography, with only the dimer exhibiting catalytic activity. Furthermore, these data suggest that the dimer−dimer contacts are critical to the catalytic integrity of the active site and may have implications concerning the relationship of *in vivo* activity and enzyme expression levels.

Overall, the quality of the electron density for both polypeptide chains in the asymmetric unit was excellent with the exceptions of several surface loops (breaks between Lys 161−Asn 167 and Ile 250−Phe 259 in subunit A and between Asp 160−Asn 167 and Lys 332−Ser 337 in subunit B). Shown in Figure 2a is a ribbon representation of the serine dehydratase dimer. It has overall dimensions of ∼100 Å × 80 Å × 60 Å and a total buried surface area of 4800 Å^2. The iron−sulfur clusters are separated by ∼25 Å. There are three *cis*-peptide bonds at Pro 15, Pro 289, and Pro 395. Both Pro 15 and Pro 289 reside approximately 10 Å from the active site, whereas Pro 395 abuts one side of the iron−sulfur cluster. Shown in Figure 2b is a stereoview of one subunit, which is distinctly bilobal in architecture. The N-terminal or β domain, delineated by Met 1−Lys 161, is dominated by a five-stranded mixed β sheet that is flanked on one side by four α helices. The C-terminal domain, which harbors the active site cluster, is composed of 11 α helices. Given that the α carbons for the two subunits of the dimer superimpose with a root-mean-square deviation of 0.25 Å, the following discussion will refer only to subunit B.

The electron density corresponding to the iron−sulfur cluster is presented in Figure 3a. Unexpectedly, the C-terminal cysteine residue, Cys 458, serves as a ligand to the iron−sulfur cluster. As indicated in Figure 3b, the C-terminal carboxylate group is hydrogen bonded into the active site via the backbone amide groups of Ser 16 and Ser 18 and the side chains of Ser 18 and Thr 290. In addition, the side chain of Ser 16 lies within hydrogen bonding distance to the carbonyl oxygen of Glu 457. Both Ser 16 and Ser 18 are part of the β domain. The other ligands to the irons are Cys 343, Cys 385, and Cys 396. Importantly, the position of Cys 458 serves as an excellent mimic for where the natural substrate, L-serine, binds as discussed further below.

Catalytic Activity with Other Amino Acids. Since the substrate of the enzyme is an amino acid, which is also thought to act as an allosteric effector, all of the other naturally encoded L-amino acids as well as D-serine and L-cystine (CysS-SsyC) were tested for their ability to act as substrates or inhibitors. Previously, L-cysteine and D-serine were reported to be competitive inhibitors of the type 2 dehydratase from *E. coli*,[8] and L-cysteine was reported to be a competitive inhibitor of the type 1 dehydratase from *P. asaccharolyticus*.[31] The only other amino acid besides L-serine that shows catalytic activity with the *L. pneumophila* enzyme studied in this investigation is L-threonine, but only at a very low level. Specifically, it exhibits approximately 3% of the level of activity seen with L-serine and shows a K_m of 288 mM compared to a K_m of 2 mM for L-serine for the wild-type enzyme. The Hill coefficient for L-threonine is 2.3 ± 0.5 compared to a value of 1.40 ± 0.04 for L-serine. The apparent cooperativity is likely due to the different affinities of the substrate for the effector and catalytic sites.

The amino acids that display significant inhibition of enzymatic activity are L-cysteine, D-serine, L-histidine, and glycine. Strikingly, L-alanine was not an effective inhibitor. Double-reciprocal plots of activity varying L-serine at fixed inhibitor concentrations are most consistent with simple competitive inhibition for L-cysteine and L-histidine with K_i values of 60 μM and 11.4 mM, respectively (Figure 4). The slope replots are linear as are plots of velocity versus inhibitor concentration, indicating that the velocity goes to zero at an infinite inhibitor concentration, which is consistent with simple competitive inhibition (Scheme 2, dashed box). Interestingly, L-cystine does not inhibit the enzyme at 1 mM and only shows approximately 12% inhibition at 20 mM.

The reciprocal plots for D-serine and glycine also appear to show competitive inhibition with apparent K_i values of 7 and 11 mM, respectively. However, the slope replot for D-serine displays a slight nonlinear character, and the plot of velocity versus inhibitor concentration shows distinct plateauing with retention of activity at higher inhibitor concentrations, indicating only partial inhibition. The plots of velocity versus glycine concentration (not shown) are not linear but do not show a distinct plateau. This along with the linear slope replot suggests that glycine inhibition is predominately competitive. Classically, partial inhibition occurs when the substrate and inhibitor bind to separate sites on the enzyme and the IES complex is capable of turning over to yield product (Scheme 2). Previous investigations have provided additional evidence of

dx.doi.org/10.1021/bi501253w | *Biochemistry* 2014, 53, 7615−7624

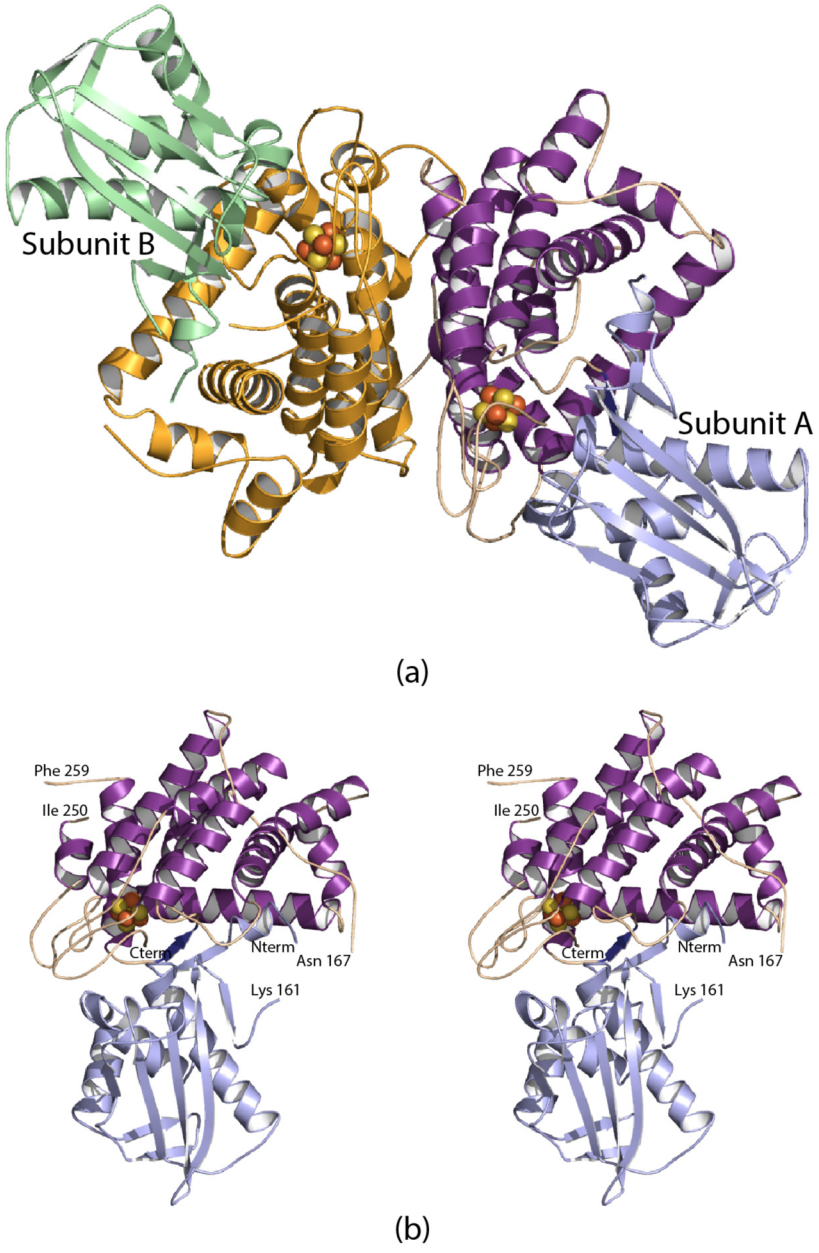

Figure 2. Structure of the *L. pneumophila* dehydratase. A ribbon representation of the dimer is presented in panel a with the metal clusters depicted in space-filling representations. A stereoview of one subunit of the enzyme is displayed in panel b. The N-terminal β-domain is colored light blue, whereas the C-terminal α domain is shown in purple. This figure and Figures 3 and 5−7 were prepared with PyMOL.[33]

two sites, a catalytic site and an effector site. The enzymatic product, pyruvate, is capable of activating the enzyme at high concentrations after initial product inhibition at lower concentrations,[14] and previous transient kinetic analyses indicate that there is a second noncatalytic site for L-serine that is responsible for activation of the enzyme.[21] Therefore, the partial inhibition observed here may be more complex than simple partial competitive inhibition, with the inhibitor and L-serine competing at two distinct sites, the catalytic and effector sites, rather than mutually exclusive sites. Scheme 2 depicts three scenarios. The central portion, in the dashed box, depicts simple competitive inhibition. The bottom portion depicts binding of the inhibitor to an allosteric site, competing with substrate activation and producing partial inhibition, and the top portion depicts substrate activation through binding to the allosteric site. If the concentration of D-serine were to increase, it would decrease the activation effect of L-serine if it was not capable of activation itself (in Scheme 2, $b > 1 > a$). The residual activity remaining at a high inhibitor concentration might reflect, at least partially, the catalytic turnover of the unactivated enzyme.

Mutational Analysis. *Possible Catalytic Residues.* The area surrounding the Fe−S cluster is occupied by a large number of polar side chains that are absolutely conserved across all four types of L-serine dehydratases. These include Ser 16, Ser 17, Ser 18, His 19, Ser 53, Thr 57, His 61, His 124, Asn 126, Ser 147, and Thr 290. In addition, Thr 63 is invariant in the type 1−3 enzymes and is a serine residue in members of the type 4 family. These conserved residues cluster together as shown in Figure 5. Note that His 61 is invariant in the type 1−3 enzymes. In members of the type 4 family that we have examined where it is missing, the proteins show no catalytic

dx.doi.org/10.1021/bi501253w | *Biochemistry* 2014, 53, 7615−7624

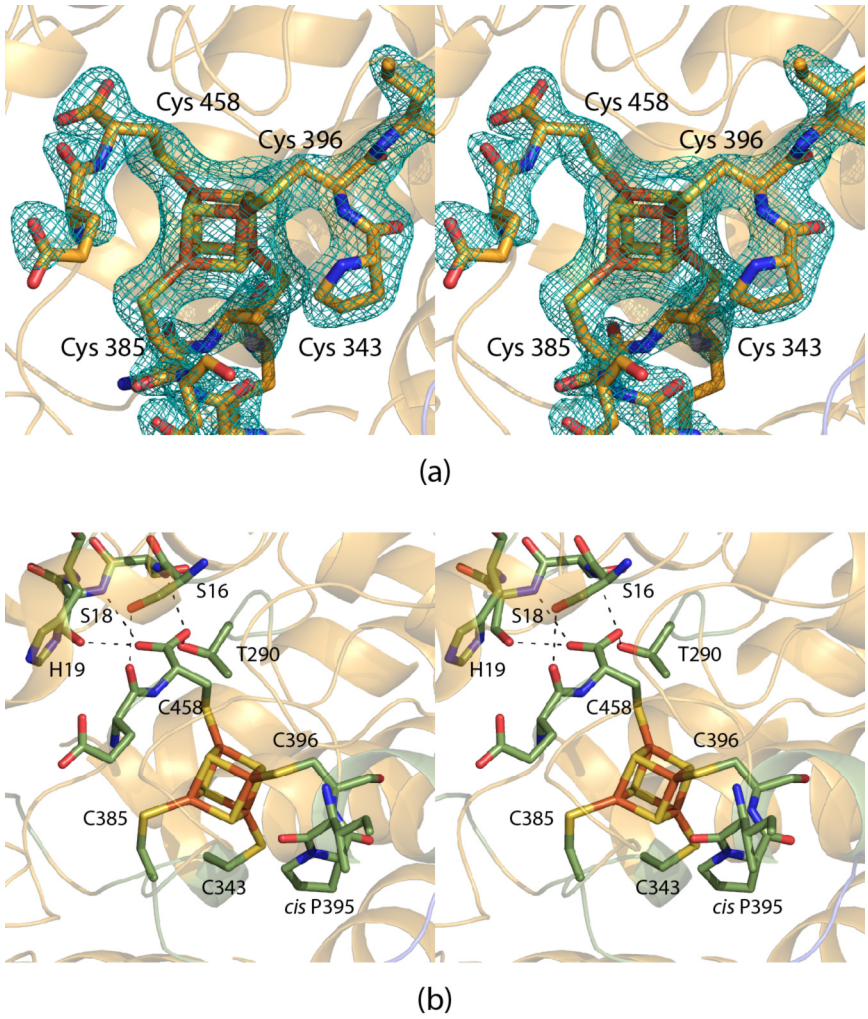

Figure 3. Active site of the *L. pneumophila* dehydratase. The observed electron density for the iron−sulfur cluster is shown in panel a. The map, contoured at 3σ, was calculated with coefficients of the form $F_0 - F_c$, where F_0 is the native structure factor amplitude and F_c the calculated structure factor amplitude. A close-up view of the active site is displayed in panel b. The dashed lines indicate potential hydrogen bonds.

activity. It is possible that the type 4 family members are pseudoenzymes because bacteria containing them always appear to express an active L-serine dehydratase, as well.

Previous mutation of Cys 458 to alanine demonstrated that there was little change in the activity of the enzyme (see Table 3).[14] Both the K_m and k_{cat} increased slightly, and the k_{cat}/K_m decreased slightly. This would indicate that the coordination of this cysteine residue to the Fe−S cluster is not essential for activity. In contrast, mutations to Cys 343, Cys 385, and Cys 396 resulted in a complete loss of activity.[14] The crystal structure confirms that these latter three cysteines form the critical structural coordination with the Fe−S cluster. As noted above, Cys 458 is anchored into the active site by multiple hydrogen bonds to its carboxylate group (Figure 3b). This hydrogen bonding pattern would still form with the alanine replacement so that the C-terminal alanine in the mutant enzyme may be performing the same function. The iron coordination by Cys 458 probably plays a key role in protecting the cluster from oxygen, which would be consistent with the relative insensitivity of the *L. pneumophila* enzyme to oxygen exposure.[17]

Clearly, Cys 458 serves as an excellent mimic for the location of the substrate, L-serine. As indicated in Scheme 1, dehydration of L-serine is assisted by extraction of the proton from its α carbon by a catalytic base. Given that there are no potential catalytic bases close enough to the α carbon of Cys 458 to perform this function in the structure described here, our current model represents a "precatalytic" conformation. There are two histidine residues (His 19 and His 61) within approximately 6 Å of the Cys 458 α carbon, however, that could possibly move within catalytic distance upon a conformational rearrangement initiated by serine binding (Figure 6). Mutation of His 61 to alanine results in a complete loss of catalytic activity. Importantly, the Fe−S cluster is still intact because the charge transfer absorbance (~400 nm) is not diminished (not shown), thus suggesting that His 61 may serve as the catalytic base. Mutation of His 19 to alanine has an effect on both K_m and k_{cat}. In addition, the mutation has a significant effect on the K_i for L-cysteine and essentially no effect on the K_i for D-serine. Most likely, His 19 is involved in substrate binding because the mutation mainly affects the interaction with the competitive inhibitor, L-cysteine.

Possible Effector Site Residues. Cys 458 is coordinated to the fourth Fe atom in the cluster, which by analogy to other 4Fe-4S proteins, such as aconitase, is expected to be the external or catalytic iron that interacts with the substrate. In addition, it is extensively hydrogen bonded, largely by residues from the β domain. It is thus likely that Cys 458 occupies the

dx.doi.org/10.1021/bi501253w | *Biochemistry* 2014, 53, 7615−7624

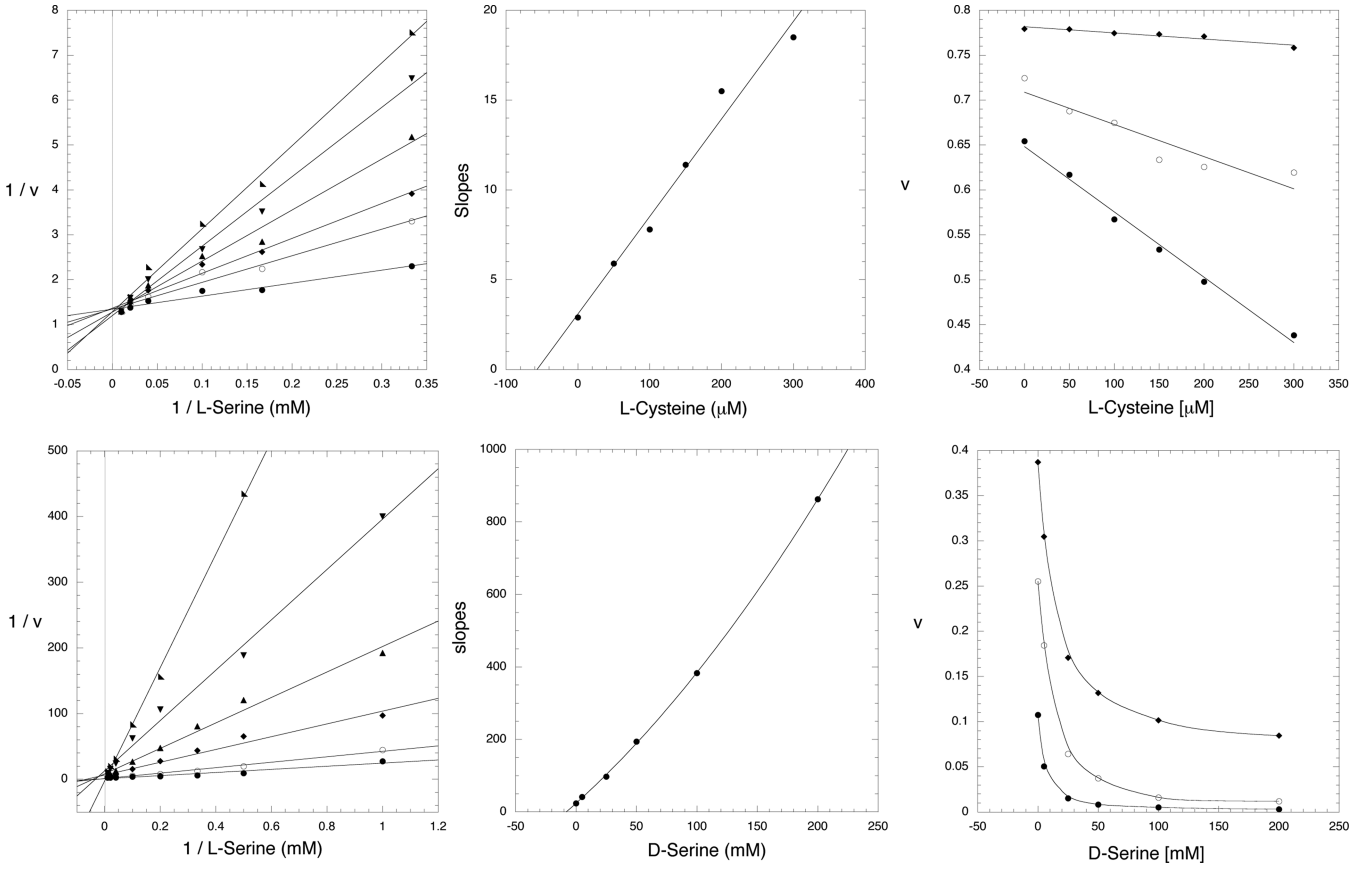

Figure 4. Inhibition kinetics of the *L. pneumophila* dehydratase with L-cysteine (top) and D-serine (bottom). For the left panels, the L-serine concentration was varied at different fixed concentrations of inhibitor and double-reciprocal plots of velocity vs L-serine concentration are shown: (top left) 0 (●), 50 (○), 100 (◆), 150 (▲), 200 (▼), and 300 (filled half-square) μM L-cysteine and (bottom left) 0 (●), 5 (○), 25 (◆), 50 (▲), 100 (▼), and 200 (filled half-square) mM D-serine. The middle panels shows slope replots of data from the double-reciprocal plots. The right panels show plots of velocity vs inhibitor concentration at fixed substrate concentrations: (top right) varying L-cysteine concentrations with 25 (●), 50 (○), and 100 (◆) mM L-serine and (bottom right) varying D-serine concentrations at 2 (●), 10 (○), and 50 (◆) mM L-serine. The *y*-axes of the double-reciprocal plots are reciprocal velocity with the velocity measured as the change in absorbance at 250 nm per minute. Double-reciprocal plots were fit by linear regression analysis that yielded values for the slopes. Slope replots and plots of velocity vs inhibitor concentration at a constant substrate concentration were fit either by linear regression analysis or in the case of D-serine to a second-degree polynomial. The values for K_i were estimated graphically from the *x*-axis intercept, which equals $-K_i$. The data points in plots of velocity vs inhibitor concentration were connected from point to point using the smooth fit function of Kaleidograph.

Scheme 2

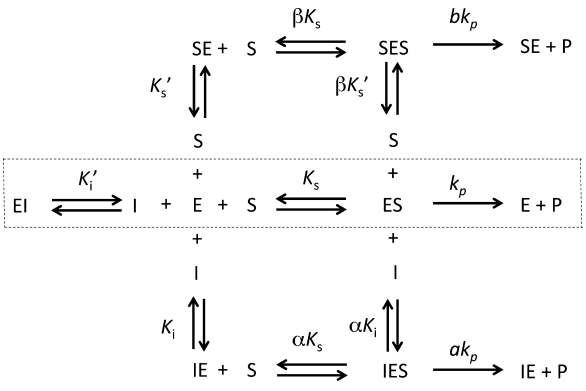

same position as the substrate or a position similar to that of the substrate when it binds to the active site. We hypothesize that activation of the enzyme by L-serine, presumably by binding to an effector site in the β domain, displaces Cys 458 and opens the active site for catalysis.

The β domain of the *L. pneumophila* dehydratase has the same structural fold as the ASB domain of D-phosphoglycerate dehydrogenase from *Mycobacterium tuberculosis,* which binds its substrate allosterically. The two domains superimpose with a root-mean-square deviation of 2.8 Å for 111 structurally equivalent α carbons. They differ significantly in two regions. As shown in Figure 7, the loops connecting the second and third α helices of the domains adopt different orientations beginning at Glu 72 in the *L. pneumophila* dehydratase. The second difference is the presence of a β hairpin motif in the β domain of the *L. pneumophila* dehydratase, which is lacking in the *M. tuberculosis* ASB domain.

By analogy to the ASB domain in D-phosphoglycerate dehydrogenase, L-serine is thought to bind to the β domain of L-serine dehydratase as an allosteric ligand. In this regard, His 124 and Asn 126 may be particularly significant. This HXN (His 124-X-Asn 126) sequence is the same motif that binds L-serine in the ACT domain of *E. coli* D-phosphoglycerate dehydrogenase (His 344-X-Asn 346). Inspection of the crystal structure of the *L. pneumophila* dehydratase shows that His 124 and Asn 126 are, indeed, in the vicinity of the active site with their side chains both pointing toward the Fe−S cluster (Figure

dx.doi.org/10.1021/bi501253w | *Biochemistry* 2014, 53, 7615−7624

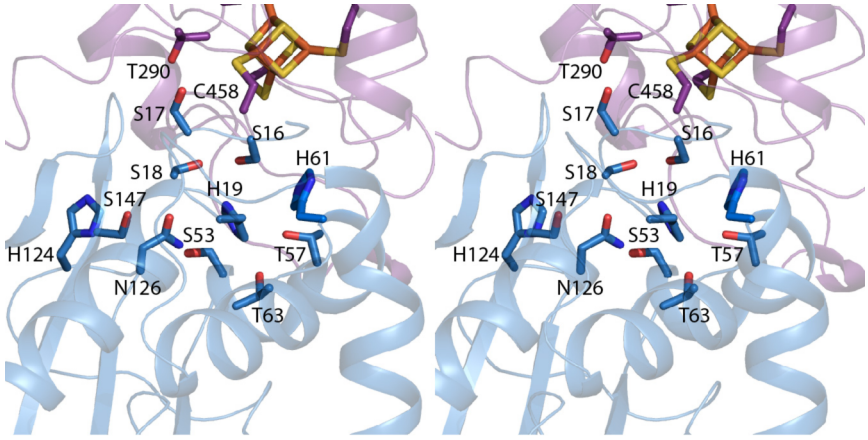

Figure 5. Cluster of conserved residues. Within the L-serine dehydratase family, there is a cluster of conserved residues located near the interface of the β and catalytic domains.

Table 3. Kinetic Parameters

enzyme	K_m (mM)	k_{cat} (s^{-1})	k_{cat}/K_m (M^{-1} s^{-1})	K_i, D-serine (mM)	K_i, L-cysteine (μM)
wild type	2.0 ± 0.1	330 ± 3	(16.5 ± 0.8) × 10^4	7	55
C458A[a]	6.9 ± 0.3	512 ± 10	(7.4 ± 0.4) × 10^4	–	–
H61A	nma[b]	nma[b]	nma[b]	–	–
H19A	24.4 ± 1.7	31 ± 1	(0.13 ± 0.01) × 10^4	8	1500
H134A/N136A	33.2 ± 2	112 ± 3	(0.34 ± 0.02) × 10^4	5.5	185

[a]From ref 14. [b]No measurable activity.

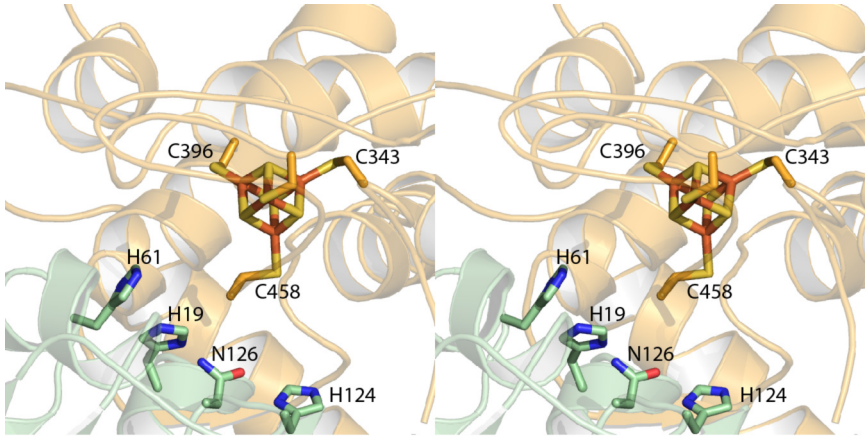

Figure 6. Possible location the allosteric binding pocket of *L. pneumophila* dehydratase. The catalytic domain is highlighted in orange, whereas the β domain is displayed in green.

6). Mutation of His 124 and Asn 126 to alanine (H124A/N126A) results in a mutant enzyme with a 17-fold higher K_m and a k_{cat} approximately one-third of that of the wild-type enzyme, resulting in a 49-fold decrease in k_{cat}/K_m (Table 3). Since the k_{cat}/K_m is essentially a second-order rate constant for ligand binding at low concentrations, this result is consistent with these residues potentially being involved with activation of the enzyme. Moreover, because they do not participate in extensive hydrogen bonding in this structure, they are poised to bind a ligand with a minimal energy cost. L-Serine may act as an effector by binding to these residues. Alternatively, L-serine may allosterically bind in a different location, causing the C-terminal Cys 458 to be released from the Fe−S cluster and subsequently to bind to His 124 and Asn 126, which could serve as a latch to prevent it from interfering with subsequent substrate binding at the active site. The inhibition constants for L-cysteine and D-serine for the *L. pneumophila* dehydratase H124A/N126A double mutant are more consistent with the latter scenario (Table 3). Whereas the K_i for D-serine actually decreases slightly, that for L-cysteine increases slightly more than 3-fold. If His 124 and Asn 126 act as a latch to tether the C-terminal cysteine away from the substrate binding pocket during catalysis, their absence would likely result in more competition at the active site for the substrate competitive inhibitor, L-cysteine. Additional data from cocrystallization and site-directed mutagenesis studies will be required to further probe the catalytic mechanism of this fascinating enzyme. These experiments are in progress.

The novel "tail in mouth" configuration revealed in this structure, where the C-terminal cysteine residue provides a unique fourth ligand to the Fe−S cluster, is typically found in the type 2 L-serine dehydratases. Other types do not usually

dx.doi.org/10.1021/bi501253w | *Biochemistry* 2014, 53, 7615−7624

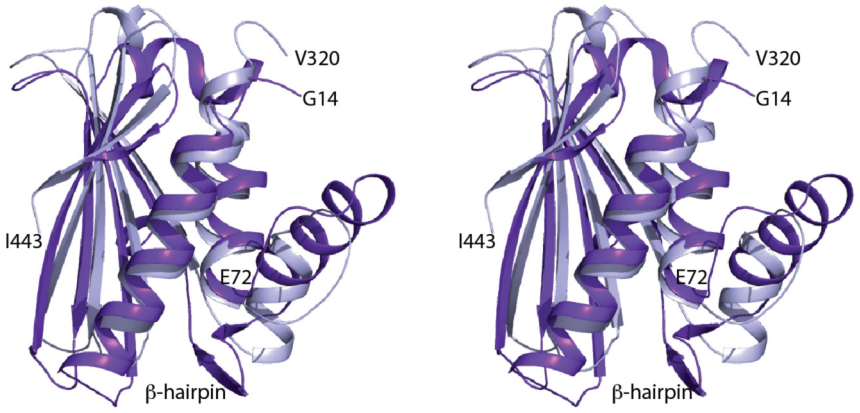

Figure 7. Comparison of the β domain to the ASB domain. Structurally, the β domain of *L. pneumophila* dehydratase is similar to the ASB domain of the *M. tuberculosis* D-phosphoglycerate dehydrogenase. Shown is a superposition of the *L. pneumophila* β domain (purple) onto the *M. tuberculosis* ASB domain (light blue). Coordinates for the *M. tuberculosis* ASB domain were obtained from the Protein Data Bank (entry 1YGY).

contain a terminal cysteine residue, although there are some that do. This suggests that its mechanism may differ in several key ways from that of the other types, including how their activity is regulated. Indeed, it has already been demonstrated that type 1 and 3 L-serine dehydratases require a monovalent cation for activity whereas the type 2 enzymes do not.[18] As far as we can tell, it appears that each bacterial species expresses only a single type of active L-serine dehydratase.[17] Furthermore, the type 1 enzymes appear to be found mainly in Gram-positive bacteria, whereas type 2 enzymes are typically observed in Gram-negative bacteria. Apparently, nature has produced several different types of Fe−S L-serine dehydratases to catalyze the same reaction with a species-specific distribution. This raises the following question: if the four types are regulated differently, is it because they are matched to some aspect of the bacterium's metabolism? This study represents a significant step toward understanding the functions of these families of enzymes and the roles that they play in the diverse lifestyles of bacteria.

■ ASSOCIATED CONTENT

Accession Codes

Coordinates have been deposited in the Protein Data Bank as entry 4RQO.

■ AUTHOR INFORMATION

Corresponding Authors

*E-mail: ggrant@wustl.edu.

*E-mail: hazel_holden@biochem.wisc.edu.

Funding

This research was supported in part by National Institutes of Health Grant DK47814 to H.M.H.

Notes

The authors declare no competing financial interest.

■ ACKNOWLEDGMENTS

A portion of the research described in this paper was performed at Argonne National Laboratory, Structural Biology Center, at the Advanced Photon Source (U.S. Department of Energy, Office of Biological and Environmental Research, supported by Contract DE-AC02-06CH11357). We gratefully acknowledge Dr. Norma E. C. Duke for assistance during the X-ray data collection at Argonne. We also thank Xiao Lan Xu for excellent technical assistance.

■ ABBREVIATIONS

CHES, *N*-cyclohexyl-2-aminoethanesulfonic acid; DEAE, diethylaminoethyl; homopipes, homopiperazine-*N*,*N*′-bis-2-ethanesulfonic acid; MOPS, 3-(*N*-morpholino)propanesulfonic acid; NTA, nitrilotriacetic acid; PCR, polymerase chain reaction; Tris, tris(hydroxymethyl)aminomethane.

■ REFERENCES

(1) Kalhan, S. C., and Hanson, R. W. (2012) Resurgence of serine: An often neglected but indispensable amino acid. *J. Biol. Chem. 287*, 19786−19791.

(2) Snell, K., and Weber, G. (1986) Enzymic imbalance in serine metabolism in rat hepatomas. *Biochem. J. 233*, 617−620.

(3) Snell, K. (1984) Enzymes of serine metabolism in normal, developing and neoplastic rat tissues. *Adv. Enzyme Regul. 22*, 325−400.

(4) Levine, E. M., and Simmonds, S. (1960) Metabolite uptake by serine glycine auxotrophs of *Escherichia coli*. *J. Biol. Chem. 235*, 2902−2909.

(5) Beremand, P. D., and Sojka, G. A. (1977) Mutational analysis of serine-glycine biosynthesis in *Rhodopseudomonas capsulata*. *J. Bacteriol. 130*, 532−534.

(6) Hama, H., Kayahara, T., Tsuda, M., and Tsuchiya, T. (1991) Inhibition of homoserine dehydrogenase I by L-serine in *Escherichia coli*. *J. Biochem. 109*, 604−608.

(7) Grabowski, R., Hofmeister, A. E., and Buckel, W. (1993) Bacterial L-serine dehydratases: A new family of enzymes containing iron-sulfur clusters. *Trends Biochem. Sci. 18*, 297−300.

(8) Cicchillo, R. M., Baker, M. A., Schnitzer, E. J., Newman, E. B., Krebs, C., and Booker, S. J. (2004) *Escherichia coli* L-serine deaminase requires a [4Fe-4S] cluster in catalysis. *J. Biol. Chem. 279*, 32418−32425.

(9) Flint, D. H., and Allen, R. M. (1996) Iron-Sulfur Proteins with Nonredox Functions. *Chem. Rev. 96*, 2315−2334.

(10) Zhang, X., and Newman, E. (2008) Deficiency in L-serine deaminase results in abnormal growth and cell division of *Escherichia coli* K-12. *Mol. Microbiol. 69*, 870−881.

(11) Zhang, X., El-Hajj, Z. W., and Newman, E. (2010) Deficiency in L-serine deaminase interferes with one-carbon metabolism and cell wall synthesis in *Escherichia coli* K-12. *J. Bacteriol. 192*, 5515−5525.

(12) Chen, J. M., Alexander, D. C., Behr, M. A., and Liu, J. (2003) *Mycobacterium bovis* BCG vaccines exhibit defects in alanine and serine catabolism. *Infect. Immun. 71*, 708−716.

(13) Velayudhan, J., Jones, M. A., Barrow, P. A., and Kelly, D. J. (2004) L-Serine catabolism via an oxygen-labile L-serine dehydratase is essential for colonization of the avian gut by *Campylobacter jejuni*. *Infect. Immun. 72*, 260−268.

(14) Xu, X. L., Chen, S., and Grant, G. A. (2011) Kinetic, mutagenic, and structural homology analysis of L-serine dehydratase from *Legionella pneumophila*. *Arch. Biochem. Biophys. 515*, 28−36.
(15) Hofmeister, A. E., Albracht, S. P., and Buckel, W. (1994) Iron-sulfur cluster-containing L-serine dehydratase from *Peptostreptococcus asaccharolyticus*: Correlation of the cluster type with enzymatic activity. *FEBS Lett. 351*, 416−418.
(16) Beinert, H., Kennedy, M. C., and Stout, C. D. (1996) Aconitase as iron-sulfur protein, enzyme, and iron-regulatory protein. *Chem. Rev. 96*, 2335−2374.
(17) Xu, X. L., and Grant, G. A. (2013) Identification and characterization of two new types of bacterial L-serine dehydratases and assessment of the function of the ACT domain. *Arch. Biochem. Biophys. 540*, 62−69.
(18) Chen, S., Xu, X. L., and Grant, G. A. (2012) Allosteric activation and contrasting properties of L-serine dehydratase types 1 and 2. *Biochemistry 51*, 5320−5328.
(19) Burton, R. L., Chen, S., Xu, X. L., and Grant, G. A. (2007) A novel mechanism for substrate inhibition in *Mycobacterium tuberculosis* D-3-phosphoglycerate dehydrogenase. *J. Biol. Chem. 282*, 31517−31524.
(20) Xu, X. L., and Grant, G. A. (2014) Regulation of *Mycobacterium tuberculosis* D-3-phosphoglycerate dehydrogenase by phosphate-modulated quaternary structure dynamics and a potential role for polyphosphate in enzyme regulation. *Biochemistry. 53*, 4239−4249.
(21) Grant, G. A. (2012) Kinetic evidence of a noncatalytic substrate binding site that regulates activity in *Legionella pneumophila* L-serine dehydratase. *Biochemistry 51*, 6961−6967.
(22) Dey, S., Burton, R. L., Grant, G. A., and Sacchettini, J. C. (2008) Structural analysis of substrate and effector binding in *Mycobacterium tuberculosis* D-3-phosphoglycerate dehydrogenase. *Biochemistry 47*, 8271−8282.
(23) Segel, I. H. (1975) *Enzyme Kinetics: Behaviour and analysis of rapid equilibrium and steady-state systems*, John Wiley & Sons, New York.
(24) Minor, W., Cymborowski, M., Otwinowski, Z., and Chruszcz, M. (2006) HKL-3000: The integration of data reduction and structure solution-from diffraction images to an initial model in minutes. *Acta Crystallogr. D62*, 859−866.
(25) Schneider, T. R., and Sheldrick, G. M. (2002) Substructure solution with SHELXD. *Acta Crystallogr. D58*, 1772−1779.
(26) Sheldrick, G. M. (2010) Experimental phasing with SHELXC/D/E: Combining chain tracing with density modification. *Acta Crystallogr. D66*, 479−485.
(27) Terwilliger, T. C. (2000) Maximum-likelihood density modification. *Acta Crystallogr. D56* (Part 8), 965−972.
(28) Terwilliger, T. C. (2003) Automated main-chain model building by template matching and iterative fragment extension. *Acta Crystallogr. D59*, 38−44.
(29) Emsley, P., and Cowtan, K. (2004) Coot: Model-building tools for molecular graphics. *Acta Crystallogr. D60*, 2126−2132.
(30) Murshudov, G. N., Vagin, A. A., and Dodson, E. J. (1997) Refinement of macromolecular structures by the maximum-likelihood method. *Acta Crystallogr. D53*, 240−255.
(31) Grabowski, R., and Buckel, W. (1991) Purification and properties of an iron-sulfur-containing and pyridoxal-phosphate-independent L-serine dehydratase from *Peptostreptococcus asaccharolyticus*. *Eur. J. Biochem. 199*, 89−94.
(32) Laskowski, R. A., Moss, D. S., and Thornton, J. M. (1993) Main-chain bond lengths and bond angles in protein structures. *J. Mol. Biol. 231*, 1049−1067.
(33) DeLano, W. L. (2002) *The PyMOL Molecular Graphics System*, DeLano Scientific, San Carlos, CA.